ARMA 21–1895

Characterization, hydraulic stimulation, and fluid circulation experiments in the Bedretto Underground Laboratory for Geosciences and Geoenergies

Hertrich, M., Brixel, B., Broeker, K., Driesner, T., Gholizadeh, N., Giardini, D., Jordan, D., Krietsch, H., Loew, S., Ma, X., Maurer, H., Nejati, M., Plenkers, K., Rast., M., Saar M., Shakas, A., van Limborgh, R., Villiger, L., Wenning, Q.C.
ETH Zurich, Zurich, Switzerland
Ciardo, F., Kaestli, P., Obermann, A., Rinaldi, A.P., Wiemer, S., Zappone, A.
Swiss Seismological Service (SED), Zurich, Switzerland
Bethmann, F., Castilla, R., Christe, F., Dyer, B., Karvounis, D., Meier, P., Serbeto, F.
Geo Energie Suisse, Zurich, Switzerland
Amann, F.
RWTW Aachen, Aachen, Germany
Gischig, V.
CSD Ingeniuere, Liebefeld, Switzerland
Valley, B.
University of Neuchatel, Neuchatel, Switzerland

This paper was prepared for presentation at the 55th US Rock Mechanics/Geomechanics Symposium held in Houston, Texas, USA, 20-23 June 2021. This paper was selected for presentation at the symposium by an ARMA Technical Program Committee based on a technical and critical review of the paper by a minimum of two technical reviewers. The material, as presented, does not necessarily reflect any position of ARMA, its officers, or members. Electronic reproduction, distribution, or storage of any part of this paper for commercial purposes without the written consent of ARMA is prohibited. Permission to reproduce in print is restricted to an abstract of not more than 200 words; illustrations may not be copied. The abstract must contain conspicuous acknowledgement of where and by whom the paper was presented.

ABSTRACT: Reservoir stimulation and hydraulic fracturing in oil-and-gas reservoirs has become common practice and the techniques are continuously improved. However, directly applying the same techniques to extract geothermal energy from low permeability crystalline rocks (i.e., *Enhanced Geothermal Systems, EGS*) continues to present operational challenges. The research community and industry have shown great interest in addressing the unresolved problems using down-scaled in-situ hydraulic stimulation experiments. Focus has been on the 1-10 m field scale, but in comparison to a realistic EGS operations (1000s m) the scale is two orders too small, the depth and associate stress field differ, and the hydraulic conditions are not perfectly representative. To study the processes in-situ and to bridge the scale between in-situ labs and actual EGS projects, the *Bedretto Underground Laboratory for Geosciences and Geoenergies* (BULGG) was built in a tunnel in the Swiss Alps so that hydraulic stimulation experiments could be performed with dense monitoring systems at the 100 m scale. This effort enables process-oriented research and testing of field scale techniques at conditions that are closer to target reservoir depths and scale. This study gives in-sight on the initial geologic, hydraulic, and stress characterization of the BULGG related to on-going stimulation and circulation experiments.

1. INTRODUCTION

Geothermal energy is considered a renewable, sustainable, and a CO_2 friendly form of power generation. The earth generates a heat flow of around 45 to 47 TW per year (Pollack et al., 1993; Davies and Davies, 2010), which is almost three times the total yearly human energy consumption (Smil, 2017; Dudley, 2019). However, the use of geothermal energy for power generation at the industrial scale has been limited to areas like tectonic boundaries and hotspots. In these preferable locations, hot rock (> 100 °C) is closer to the surface where permeabilities are naturally high enough (~ 10^{-16} m^2), making heat extraction by means of cold surface water injection and hot water extraction economically viable. As societies and politics dictate transitions to carbon neutral and carbon negative energy sources, many countries are expanding efforts to extract geothermal energy from deeper naturally occurring heat sources

by means of 'Enhanced Geothermal Systems' (EGS), previously known as 'petrothermal' or 'hot dry rock geothermal' energy.

As the name suggests, these systems need to be 'enhanced' by means of hydraulic stimulation or fracturing to achieve a sufficient permeability that enables economic heat extraction. These EGS reservoir stimulations are generally expected to occur at depths of 3 to 6 km, which adds extra difficulties, not only in the in the increased financial cost of drilling and completions, but also in engineering the heat extraction at such depths. To date there are, in comparison to the oil-and-gas industry, just a few industrial scale projects that provide learning experiences for this 'underdeveloped' technology. Some examples from across the globe include: Fenton Hill and FORGE, USA (Brown, 1995; Albright and Pearson, 1982; Moore et al., 2018), Haute-Sorne, Switzerland (Link et al., 2020), and Soultz-sous-Forets, France (Genter et al., 2010).

Past experience has shown it is difficult and nearly unpredictable to establish a hydraulically connected heat exchanger, while keeping induced seismicity at an acceptable level (Ghassemi, 2012; Grigoli et al., 2018; Lee et al., 2019). To tackle these unresolved problems, the research community and industry have implemented scaled-down in-situ hydraulic stimulation experiments in representative rocks (Amann et al., 2017; Zimmerman et al., 2019; Oldenburg, et al., 2020). The practical and economic benefit of such experiments is the ability to surround a smaller target stimulation volume (1 to 10 m^3) with a dense array of sensors (seismometers, acoustic emissions, fiber optics – distributed strain and temperature, etc.) and have precise controls on the natural conditions, as well as fluid volumes and rates injected and produced. The downside is that these experiments are often done close to the surface at scales of two orders of magnitude smaller than industrial EGS (1000s m^3), where the depth and associated stress field differ, and the hydraulic conditions are not perfectly representative.

To study the processes in-situ and to bridge the scale between in-situ labs and actual EGS projects, the *Bedretto Underground Laboratory for Geosciences and Geoenergies* (BULGG) was built in an existing abandoned tunnel in the Swiss Alps so that hydraulic stimulation experiments could be performed with dense monitoring systems at the 100 m scale. The BULGG enables process-oriented research and testing of field scale techniques with industry partners at conditions that are closer to target reservoir depths and scale.

Since 2017, several field mapping and drilling campaigns have focused on characterizing the geology, structures, and stresses along the tunnel and in short boreholes (< 30 m) along the tunnel (Gischig et al., 2020). Over the course of the last year, a series of boreholes 100 to 400 m long were drilled in the 'laboratory' section of the BULGG that intersect several fault zones that are being used to emulate an EGS reservoir. Four of these boreholes were drilled to establish a monitoring network around two stimulation boreholes.

This contribution presents the results to date of the on-going reservoir characterization, stimulation, and circulation experiments. We report the geologic system, stress state, and hydraulic properties prior to stimulation. We also present preliminary results of the on-going stimulation of the reservoir.

2. GEOLOGIC SETTING

The Bedretto Laboratory or BULGG is located in an access tunnel to the Furka base railway tunnel in the Gotthard Massif in south central Switzerland (Fig. 1). The Gotthard Massif trends NE-SW and was thrust northwards during the Alpine orogenesis (Labhart, 2005; Berger et al., 2017; Herwegh et al., 2017; Rast, 2020). The tunnel trends NW-SE and penetrates three consecutive geologic units: 1) the Tremola series from ca. 0 to 434 TM (tunnel meter, measured from the southern portal), 2) the Prato series from 434 to 1138 TM, and 3) the Rotondo granite from 1138 TM to the end of the tunnel at 5218 TM (Schneider, 1985; Rast, 2020). The tunnel is unlined throughout most of the tunnel, with the exception of several groundwater inflow zones that are localized in fault zones along the tunnel.

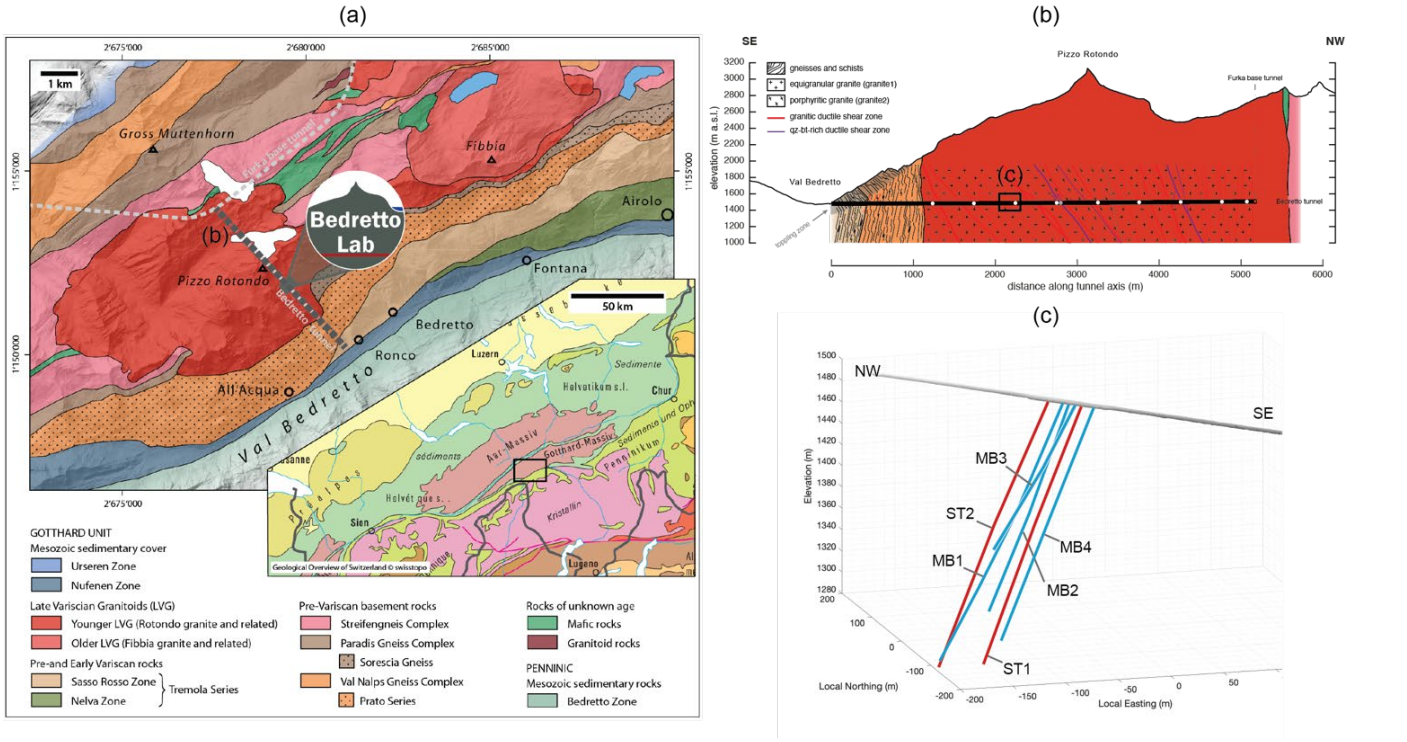

Fig. 1. (a) Geological overview of the study area (Bedretto tunnel), compiled after: Hafner et al., 1975; Berger et al., 2016; Federal Office of Topography swisstopo, 2016; Rast, 2020. (b) Cross section: geology along the tunnel axis compiled after: Keller and Schneider, 1982; Rast, 2020. (c) Boreholes drilled for stimulation (ST) and monitoring (MB) from within the BULGG.

The majority of drilling activities in the BULGG have been concentrated around an enlarged niche in the tunnel from 2000 to 2100 TM, which is entirely inside the Rotondo granite, where the overburden is ca. 1040 to 1080 m. The intrusion age of the Rotondo granite is 294 ± 1.1 Ma, making it slightly younger than the Fibbia granite that intruded into the Gotthard massif a few kilometers to the NE 299 ± 1.2 Ma (Sergeev et al., 1995).

The Rotondo granite is primarily massive, equigranular and fine-grained (aplitic) with a mineral content of quartz (25 to 35%), K-feldspar (20 to 40%), plagioclase (10 to 25%), biotite (3 to 8%) and trace amounts of garnet, phengite, chlorite and other accessory minerals (Hafner, 1958; Labhart, 2005). The Bedretto granite generally develops weak foliation in some parts of the tunnel (Lutzenkirchen and Loew, 2011) and ductile deformation is concentrated around distributed shear zones along the tunnel (Schneider, 1985). The ductile shear zones are typically granitic (G-DSZ) with similar composition to the host granite or quartz-biotite-rich (QB-DSZ) and both types are similarly oriented (Rast, 2020). In contrast to the Fibbia granite, the foliation is less pervasive and more localized in the Rotondo granite (Schneider, 1985; Lutzenkirchen and Loew, 2011), and are interpreted to form as a result of progressive Alpine deformation (Marquer, 1990). However, other studies suggest that the more pervasive foliation in the Fibbia and other granites within the Gotthard Massif formed during a late Variscan deformation phase before the intrusion of the younger Rotondo granite (Guerrot and Steiger, 1991).

Regardless of the timing, the ductile shear zones within the Rotondo granite localized brittle deformation during the later stages of the Alpine orogeny (Lutzenkirchen and Loew, 2011), which can have a loss of cohesion within the damage zone (Schneider, 1985). The brittle deformation in the Rotondo granite is estimated to occur between 18 and 14 Ma at temperatures of 200 to 300 °C (Lützenkirchen and Loew, 2011).

Table 1. List of monitoring and stimulation boreholes. All depths are total drilled depth. MB3 has the deepest installation depth due to borehole stability blockage in (*).

Borehole	Depth [m]	Usage and measurement system
MB1	300	Cemented: Geophone, AE sensors (trans./rec.), Temp/Strain FO, FBG
MB2	219	Pseudo-permanent: Six interval multi-packer fluid pressure monitoring system
MB3	192 (160*)	Cemented: Geophone, AE sensors (trans./rec.), Temp/Strain FO
MB4	250	Cemented: Geophone, AE sensors (trans./rec.), Temp/Strain FO
ST1	399	Open hole: packers and/or geophone string
ST2	349	Open hole: packers and/or geophone string (evtl. perforated casing)

3. BULGG RESERVOIR BOREHOLE GEOMETRY AND USAGE

Within the enlarged niche in the tunnel from 2000 to 2100 TM, a series of four monitoring (MB) and two stimulation (ST) boreholes were drilled that intersect several fault zones. The boreholes were drilled along the southwestern tunnel wall dipping ca. 45 degrees and have lengths ranging from 192 to 399 m (Fig. 1 and Table 1).

Three monitoring boreholes (MB1, 3 and 4) have a diameter of 6.5 inch (16.5 cm) and are equipped with a geophone at the base, a string of acoustic emission (AE) sensors, an acoustic transmitter source, and temperature and strain fiber optic (FO) spanning the length of the borehole. MB1 has additional local Fiber Bragg Gratings (FBG) strain sensors. All sensors are cemented in place. MB2 is equipped with a multi-packer system that enables pseudo-permanent monitoring of the fluid pressure in six intervals along the borehole. The stimulation boreholes (ST1 and ST2) have a diameter of 8.5 inch (21.6 cm) and are open without casing. The stimulation boreholes are left open so that either can be used as the stimulation borehole with a double or multi-packer system or to monitor using a geophone string.

4. RESERVOIR CHARACTERIZATION

4.1. Geology and Structures

The geologic characterization of the rock volume utilizes a combination of core mapping and acoustic and optical televiewer logs (ATV/OTV) from the MB and ST boreholes. Seismic tomography and ground penetrating radar tomography (e.g., Shakas et al., 2020) aids in tracing these structures across the volume. The predominant geology within the reservoir volume is weakly deformed Rotondo granite protolith, where foliation is generally not recognizable at the hand specimen scale, and distributed ductile shear zones and brittle fault zones. Other structures include: non-filled and filled fractures, dikes and veins, and compositional foliation within the granite, which usually occurs in the vicinity of the ductile shear zones.

The reservoir volume can be broken up into four units based on the distribution and orientation of structures (Castilla et al., 2020). In the shallow section (down to ca. 60 to 120 m measured depth, MD, depending on borehole), there are few isolated fractures, shear zones, and dykes, but in general the granite is intact.

The beginning of the second and third unit is marked by the first prominent shear zone is encountered at 60 to 120 m MD (Fig. 2), whose trajectory can be traced back to a predominant shear zone along the tunnel at ca. 1980 TM. The differences between these units is based on the predominant fault orientation. The top of this more fractured and foliated middle unit is clearly identified on OTV and ATV logs as a ca. 1 to 2 m thick fracture zone where the borehole wall is washed out over the entire interval (Fig. 2). Right above this opening, the core confirms the foliation with increased quartz and biotite composition, similar to the QB-DSZ observed along the tunnel (cf. Rast, 2020). Core recovery from the fault zone is about ca. 50 %. After this fault zone, we encounter several highly foliated ductile shear zones and brittle fault zones. There is also an increase in isolated fractures. The brittle fault zones occur in swarms and often the area around these features is washed out as seen in ATV and borehole camera images (Fig. 2). The brittle fault zones appear to occur primarily along precursory ductile shear zones since their orientations are similar (Fig. 2e-f). The brittle fault zones, which often overprint the inherited ductile structure, have less cohesive fault gouge and cataclastic fault cores. The ductile shear zones are

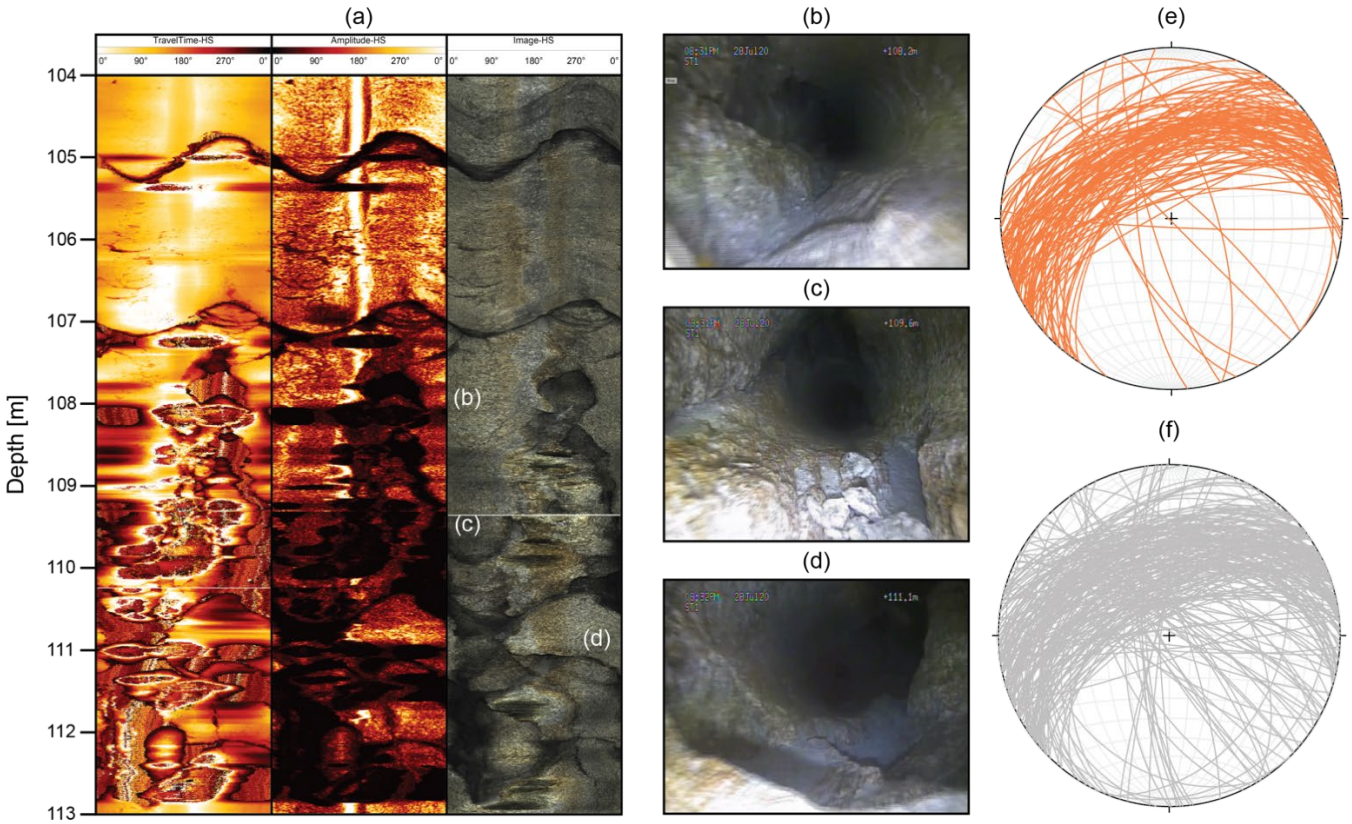

Fig. 2. (a) Example acoustic and optical televiewer logs in ST1 depicting the fracture zone that signifies the start of the highly fractured zones. (b-d) Borehole camera images of the fracture and washout zones shown in the logs in 'a'. (e) Stereonet projection of the ductile shear zone orientations along the borehole. (f) Stereonet projection of the non-filled fractures along the borehole.

characterized as mylonites to ultramylonites that have sub-millimeter foliations which can form as a strain gradient with increasing foliation spacing and grain size spanning a couple of meters in thickness or can occur as an abrupt strain localization feature of a couple to tens of cm in thickness. Both the ductile shear zones and the brittle faults zones are composed of multiple branches of anastomosing individual fault cores.

After about 100 m of this highly fractured and deformed unit, deformation again becomes less pronounced and occurs again as discrete features, marking the beginning of the fourth unit. The granite is again more intact over distances of several 10s of meters.

4.2. In-situ stresses

We conducted small scale hydraulic fracturing tests, so-called mini-frac tests (Haimson and Cornet, 2003), to estimate the local stress field and its spatial variability. The tests were performed in over 40 intact rock intervals in the six short SB boreholes (30 m to 40 m long) and borehole MB1 (300 m long, deviated). The observed hydraulic fracture traces are steeply-dipping on acoustic and optical televiewer logs, which generally validates the assumption of the overburden or vertical stress (S_v) being a principal stress direction. The inferred direction of the maximum horizontal stress (S_{Hmax}) is approximately WNW-ESE (Ma et al., 2020). We compared different techniques to estimate the minimum horizontal stress magnitude (S_{hmin}) and its uncertainty for the initial stress measurement campaign in the short SB boreholes (Bröker, 2019; Bröker and Ma, 2021). The inferred stress magnitudes are: S_{hmin} = 11.2 to 16.4 MPa, S_{Hmax} = 19.8 to 27.6 MPa, $S_v \approx$ 26.5 MPa (Fig. 3). Our results confirm that the stress state in the vicinity of the Bedretto Lab is transitional between normal and strike-slip faulting ($S_v \geq S_{Hmax} > S_{hmin}$). This agrees well with the regional stress field (Kastrup et al., 2004; Heidbach et al., 2016) and stress-induced failures (e.g., spalling and kinking) observed along sections of the Bedretto Tunnel (Gischig et al., 2020; Ma et al., 2020). Extended shut-in times up to 15 hours were used to obtain the local pore pressure (P_p). It ranges from 2.0 to 5.6 MPa, reflecting strong tunnel drainage and pressure drawdown.

Deeper mini-frac intervals in the long MB1 borehole yield breakdown pressures comparable to the ones

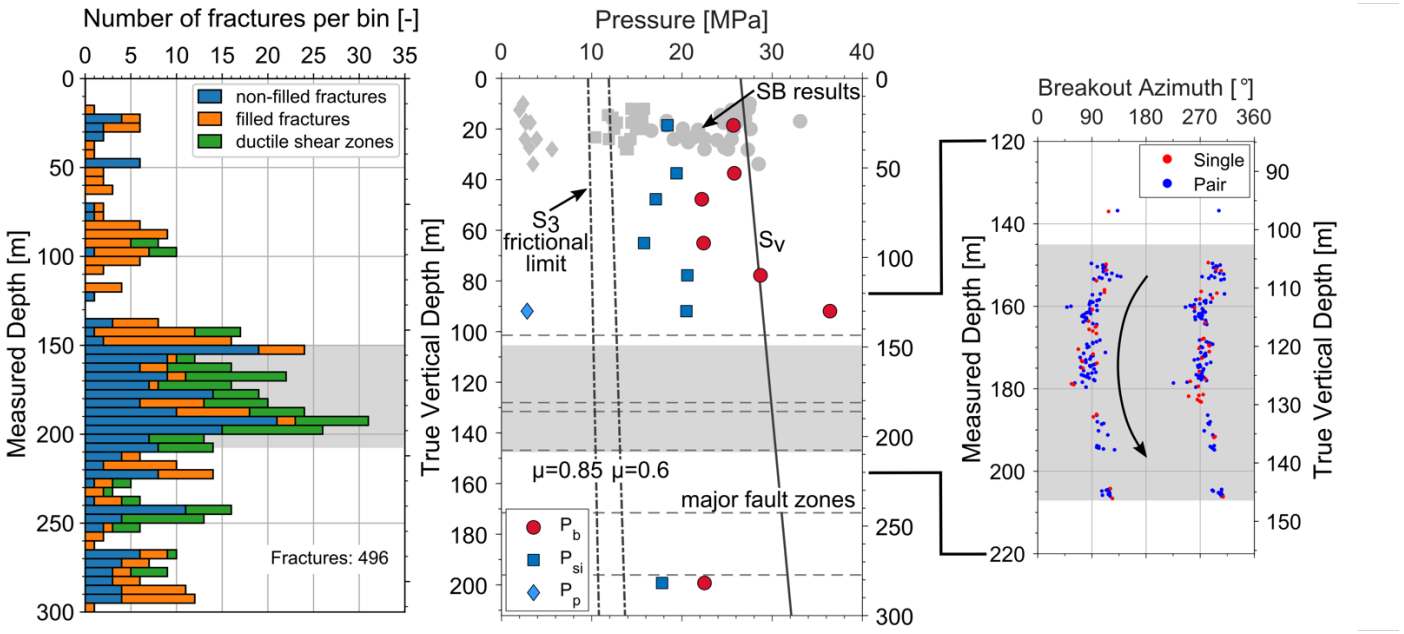

Fig. 3. (left) Histogram of the mapped fractures observed in MB1. (middle) Results of the mini-frac stress measurements in MB1: The P_{si} (instantaneous shut-in pressure) gives an upper bound of the minimum horizontal stress magnitude. P_b denotes the breakdown pressure and P_p the measured pore pressures. The vertical stress magnitude is calculated from the overburden and the lower limit of the minimum horizontal stress from frictional equilibrium theory (assuming P_p = 5 MPa and a frictional coefficient of 0.6 or 0.85). (right) Close-up to the zone where breakouts occur in MB1. Single breakouts and breakout pairs are indicated with respect to the top of the borehole (high side).

measured close to the Bedretto Lab, but the derived minimum horizontal stress magnitude follows a higher gradient (Fig. 3). We attribute such discrepancies to stress perturbations in the vicinity of the tunnel and compartmentalized hydro-structures connected to major fault zones.

Another feature in the long boreholes is the appearance of breakouts, which were mapped and analyzed to have a second estimate of the in-situ stress field (van Limborgh, 2020). The breakout azimuths show a rotation of 40° with a wavelength of about 40 m (Fig. 3). This rotation indicates that the stress field is perturbed by the presence of fractures in this zone. Preliminary modelling shows that the breakout azimuth corresponds to a S_{Hmax} azimuth between E and SE, which is consistent with the mini-frac results.

4.3. Hydraulic properties

A series of hydraulic tests was carried out prior to cementing the monitoring system in the MB1 to 3 to characterize the transmissivity in several locations along the borehole. A similar set of measurements was performed in ST1 and ST2. Both sets of experiments utilized a double or multi-packer assembly to isolate the different zones for drawdown or injection testing.

All tests were carried as a 'single hole' measurement from a starting pore pressure of ca. 4.0 MPa. The drawdown and injection curves were analyzed using both the methods for hydraulic tests by Theis, 1935 and Barker, 1988. In general, both methods give similar estimates with the Theis, 1935 method being up to a half of an order of magnitude higher than Barker, 1988. The hydraulic testing in the MB boreholes shows a very heterogeneous system, with transmissivity ranging from 10^{-11} to 10^{-6} [m^2/s], with the highest values occurring in the intervals with a high density of fractures. Hydraulic testing in the ST boreholes falls within this range. Cross hole monitoring of pressure changes in the other boreholes also shows a heterogenous response, and a systematic pattern has yet to be unraveled.

5. STIMULATION

The deepest sections of ST1 and ST2 were stimulated from November to December 2020 using a double packer system. Several intervals of interest were chosen based on observed natural fractures and zones that had been notched a priori. The stimulation followed a strict 'Traffic Light System' that utilized seismic magnitude, ground motion, and pressure monitoring to limit and mitigate the seismic risk of

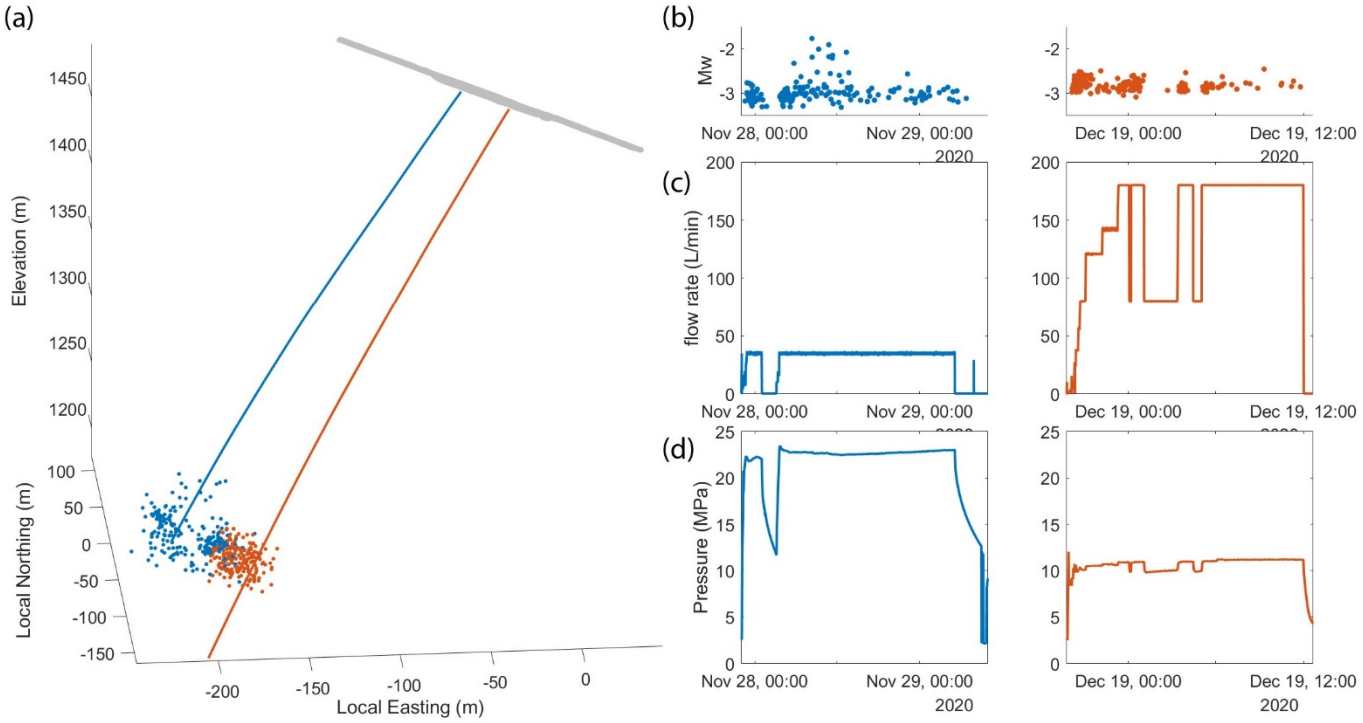

Fig. 4. (a) Boreholes ST1 (red) and ST2 (blue) and their associated seismic event distribution during stimulation of two intervals. (b) Moment magnitude of events during the injection time period. (c) Flow rate during the stimulation. (d) Fluid pressure in the injection intervals (as measured from the wellhead).

the stimulation. These are beyond the scope of this conference paper, where we focus on the results from the stimulation of an interval in ST1 and in ST2. The following results come from the data that was acquired real-time during the stimulation. Therefore, the seismic events have not been re-evaluated or re-processed to improve the uncertainty of the localization, and potential by-pass in the pressure and flow rate data has not been evaluated.

Fig. 4 shows the ST1 (red) and ST2 (blue) boreholes with the induced seismicity cloud for each respective borehole in space, the distribution of magnitude of the events through time, and the associated pressure and flow rate data. The stimulation in ST2 (Nov. 19, 2020: borehole depth 319 to 325 m) and the stimulation in ST1 (Dec. 19, 2020: borehole depth 336 to 344 m) targeted preexisting natural fractures within the stimulated intervals. There were about 700 to 900 total seismic events recorded during the stimulation in each interval, of which 197 and 208 seismic events could be localized and given a magnitude in ST1 and ST2, respectively.

The stimulation in ST2 was limited by the pumps to have a maximum of ca. 47 L/min injection rate, which generated a fluid pressure of 22 to 23 MPa (measured at the wellhead). The moment magnitude of all events was between -3.5 and -1.9 Mw. A new set of pumps were installed that enabled higher flow rates during the stimulation of ST1. Despite nearly quadrupling the flow rate (sustained injection of ca. 175 L/min) the measured fluid pressure during injection was only ca. 10 to 12 MPa and the moment magnitude of all events ranged between -3.1 and -2.5 Mw. The seismic cloud distribution shows overlap in the event distribution between the two boreholes.

6. DISCUSSION AND SUMMARY

The experiments to date in the BULGG builds upon the foundation of smaller scale in-situ experiments (e.g., Amann et al., 2017; Zimmerman et al., 2019), which lead to a better understand how the natural conditions and engineering technology effect reservoir stimulation in EGS reservoirs. Over the course of the next several years several experiments will focus on 1) how to stimulate and create large reservoir volumes while keeping induced seismicity under control, 2) earthquake source processes and variability of aseismic and seismic deformation, 3) how to create an economic heat exchanger, and 4) the

development of drilling, completion, and production technologies for economic multi-stage simulations in EGS projects.

The vast monitoring network and characterization will enable us to study the hydromechanical response of the reservoir to stimulation, circulation, and production of fluids to create a sufficient heat exchanger. This is done by utilizing the dense network of complementary monitoring sensors and extensive characterization of the natural and induced structures in the reservoir. With this monitoring network we will be able to have an accurate detection of seismic events, and how they are related to the interaction of geologic structures and in-situ stresses within the 'reservoir'. Fig. 3 shows that the brittle fractures occur together with the ductile shear zones, which also correlates with the zone of increase borehole breakouts. As these zones are stimulated we will be able to understand how these pre-existing natural structures interact with hydraulic fractures and the in-situ stresses with strain and temperature fiber optic sensing. We will be able to monitor the spatial, temporal, and magnitude variability of induced seismicity with the acoustic emission, distributed acoustic fiber optic sensors, and geophones. We will monitor the pore pressure changes across the reservoir. All of these characterization and monitoring will ultimately lead to a more complete understanding of the hydromechanical response of the rock mass and encompassing fractures under EGS deformation conditions.

ACKNOWLEDGEMENTS

The Bedretto Underground Laboratory for Geosciences and Geoenergy is an ETH infrastructure and is financed by ETH Immobilien. The Bedretto Lab experiments are funded by the Swiss Federal Office of Energy (SFOE) (project VALTER), by the EU Horizon 2020 (project DESTRESS), by the EU initiative Geothermica – EraNet (project ZoDrEx and project SPINE), the Werner von Siemens Stiftung (project MISS) and by ERC (project FEAR). The Bedretto tunnel is property of the Matterhorn Gotthard Bahnen (MGB).

REFERENCES

Albright, J.N. and Pearson, C.F., 1982. Acoustic emissions as a tool for hydraulic fracture location: Experience at the Fenton Hill Hot Dry Rock site. *Society of Petroleum Engineers Journal*, *22*(04), pp.523-530.

Amann, F., Gischig, V., Evans, K., Doetsch, J., Jalali, R., Valley, B., Krietsch, H., Dutler, N., Villiger, L., Brixel, B. and Klepikova, M. 2018. The seismo-hydromechanical behavior during deep geothermal reservoir stimulations: open questions tackled in a decameter-scale in situ stimulation experiment. *Solid Earth*, *9*(1), pp.115-137.

Barker, J.A. 1988. A generalized radial flow model for hydraulic tests in fractured rock. *Water Resources Research*, *24*(10), pp.1796-1804.

Berger, A., Mercolli, I. P., Herwegh, M., and Gnos, E. (2017). Explanatory Notes to the Geological map of the Aar massif, Tavetsch and Gotthard nappes, Geological special map No. 129. *Federal Office of Topography swisstopo*, Wabern.

Bröker, K. 2019. In-Situ Stress and Rock Mass Characterization via Mini-Frac Tests at the Bedretto Underground Laboratory. Master's Thesis. *ETH Zurich*. https://doi.org/10.3929/ethz-b-000445278.

Bröker, K. and X. Ma (2021). Estimating the least principal stress in a granitic rock mass: systematic mini-frac tests and elaborated pressure transient analysis. *Submitted to Rock Mechanics and Rock Engineering*. https://www.research-collection.ethz.ch/handle/20.500.11850/466482

Brown, D., 1995, May. The US hot dry rock program—20 years of experience in reservoir testing. In *Proceedings of the world geothermal congress, Florence, Italy* (Vol. 4, pp. 2607-2611).

Castilla, R., Krietsch, H., Jordan, D., Ma, X., Serbeto, F., Shakas, A., Guntli, P., Bröker, K., Löw, S., Hertrich, M. and Bethmann, F., 2020, December. Conceptual Geological Model of the Bedretto Underground Laboratory for Geoenergies. In *82nd EAGE Annual Conference & Exhibition* (Vol. 2020, No. 1, pp. 1-5). European Association of Geoscientists & Engineers.

Davies, J.H. and D.R. Davies. 2010. Earth's surface heat flux. *Solid Earth*, 1, 5-24. https://doi.org/10.5194/se-1-5-2010

Dudley, B. 2019. BP Statistical Review of World Energy. 68th edition. London, UK, accessed Jan., 15, 2021.

Federal Office of Topography swisstopo (2016). Geological Overview of Switzernland. Retrieved from https://shop.swisstopo.admin.ch/en/products/accessories/postcards, Date Accessed: 2020-01-14.

Genter, A., Evans, K., Cuenot, N., Fritsch, D. and Sanjuan, B., 2010. Contribution of the exploration of deep crystalline fractured reservoir of Soultz to the knowledge of enhanced geothermal systems (EGS). *Comptes Rendus Geoscience*, *342*(7-8), pp.502-516.

Ghassemi, A., 2012. A review of some rock mechanics issues in geothermal reservoir development. *Geotechnical and Geological Engineering*, *30*(3), pp.647-664.

Gischig, V.S., Giardini, D., Amann, F., Hertrich, M., Krietsch, H., Loew, S., Maurer, H., Villiger, L., Wiemer, S., Bethmann,

F. and Brixel, B., 2020. Hydraulic stimulation and fluid circulation experiments in underground laboratories: Stepping up the scale towards engineered geothermal systems. *Geomechanics for Energy and the Environment*, *24*, p.100175.

Grigoli, F., Cesca, S., Rinaldi, A.P., Manconi, A., Lopez-Comino, J.A., Clinton, J.F., Westaway, R., Cauzzi, C., Dahm, T. and Wiemer, S., 2018. The November 2017 Mw 5.5 Pohang earthquake: A possible case of induced seismicity in South Korea. *Science*, *360*(6392), pp.1003-1006.

Guerrot, C. and Steiger, R. H. 1991. Variscan granitoids in the Gotthard-massif, Switzerland: Pb-U single zircon and Sr-Nd data. *Terra abstracts*, 3(1):35.

Hafner, S., 1958. *Petrographie des südwestlichen Gotthardmassivs zwischen St. Gotthardpass und Nufenenpass* (Doctoral dissertation, ETH Zurich).

Haimson, B.C. and F.H. Cornet. 2003. ISRM suggested methods for rock stress estimation-part 3: Hydraulic fracturing (HF) and/or hydraulic testing of pre-existing fractures (HTPF). *International Journal of Rock Mechanics and Mining Sciences*. 40(7-8): 1011-1020.

Heidbach O., Rajabi M., Reiter K., Ziegler M., WSM Team. 2016. World stress map database release 2016. *GFZ Data Services*. http://doi.org/10.5880/WSM.2016.001

Herwegh, M., Berger, A., Baumberger, R., Wehrens, P., and Kissling, E. (2017). Large-Scale Crustal-Block-Extrusion During Late Alpine Collision. *Scientific Reports*, 7(1):1–10.

Kastrup, U., Zoback, M. L., Deichmann, N., Evans, K. F., Giardini, D., & Michael, A. J. (2004). Stress field variations in the Swiss Alps and the northern Alpine foreland derived from inversion of fault plane solutions. *Journal of Geophysical Research-Solid Earth*, 109(B1). https://doi.org/Artn B01402 Doi 10.1029/2003jb002550

Labhart, T. P. 2005. Erläuterungen zum Geologischen Atlas der Schweiz 1:25000, Val Bedretto, Atlasblatt 68. Bundesamt für Wasser und Geologie, Bern-Ittigen.

Lee, K.K., Ellsworth, W.L., Giardini, D., Townend, J., Ge, S., Shimamoto, T., Yeo, I.W., Kang, T.S., Rhie, J., Sheen, D.H. and Chang, C., 2019. Managing injection-induced seismic risks. *Science*, *364*(6442), pp.730-732.

Link, K., Lupi, N. and Siddiqi, G., 2020. Geothermal Energy in Switzerland–Country Update 2015-2020. In *Proceedings, World Geothermal Congress 2020, Reykjavik* (p. 16).

Lützenkirchen, V. and Loew, S., 2011. Late Alpine brittle faulting in the Rotondo granite (Switzerland): deformation mechanisms and fault evolution. *Swiss Journal of Geosciences*, *104*(1), pp.31-54.

Ma X., Doonechaly N. G., Hertrich M., Gischig V. & Klee G. 2019. Preliminary in situ stress and fracture characterization in the Bedretto Underground Laboratory, Swiss Alps: implications on hydraulic stimulation. In: Rock Mechanics for Natural Resources and Infrastructure Development - *Full Papers Proceedings of the 14th International Congress on Rock Mechanics and Rock Engineering* (ISRM 2019), September 13-18, 2019, Foz do Iguassu, Brazil.

Marquer, D. 1990. Structure et déformation alpine dans les granites hercyniens du massif du Gothard (Alpes centrales suisses*). Eclogae Geologicae Helvetiae*, 83(1):77–97.

Moore, J., Allis, R., Pankow, K., Simmons, S., McLennan, J., Rickard, W., Gwynn, M. and Podgorney, R., The Utah FORGE Site: A Laboratory for Enhanced Geothermal System Development. In *AAPG ACE 2018*.

Oldenburg, C, Dobson, P., Wu, Y., Cook, P., Kneafsey, T., Nakagawa, S., et al., 2020. Hydraulic fracturing experiments at 1500 m depth in a deep mine: Highlights from the kISMET project. United States. *Web*.

Pollack, H. N., S.J. Hurter, and J.R., Johnson. 1993. Heat flow from the Earth's interior: Analysis of the global data set. *Rev. Geophys.*, 31(3), 267– 280, doi:10.1029/93RG01249.

Rast, M. 2020. Geology, Geochronology and Rock Magnetics Along Bedretto Tunnel (Gotthard Massif, Central Alps) and Numerical Modelling of Quartz-Biotite Aggregates. MSc Thesis, *ETH Zurich*.

Schaltegger, U. and Corfu, F., 1992. The age and source of late Hercynian magmatism in the central Alps: evidence from precise U− Pb ages and initial Hf isotopes. *Contributions to Mineralogy and Petrology*, *111*(3), pp.329-344.

Schneider, T. 1985. Basistunnel Furka - Geologische Aufnahme des Fensters Bedretto. Technical Report, *Furka-Oberalp-Bahn AG*, Brig.

Sergeev, S. A., Meier, M., and Steiger, R. H. (1995). Improving the resolution of single-grain U/Pb dating by use of zircon extracted from feldspar: Application to the Variscan magmatic cycle in the central Alps. *Earth and Planetary Science Letters*, 134(1-2):37–51.

Shakas, A., Maurer, H., Giertzuch, P.L., Hertrich, M., Giardini, D., Serbeto, F. and Meier, P., 2020. Permeability enhancement from a hydraulic stimulation imaged with Ground Penetrating Radar. *Geophysical Research Letters*, *47*(17), p.e2020GL088783.

Smil, V., 2016. *Energy transitions: global and national perspectives* ABC-CLIO.

Theis, C. V. 1935. The relation between the lowering of the piezometric surface and the rate and duration of discharge of a well using ground-water storage. *Eos, Transactions American Geophysical Union*, *16*(2), 519-524.

van Limborgh, R. 2020. Borehole Indicators of In Situ Stress Field Heterogeneity at the Bedretto Underground Laboratory. Master's Thesis. *ETH Zurich*. https://doi.org/10.3929/ethz-b-000445987

Zimmermann, G., Zang, A., Stephansson, O., Klee, G. and Semiková, H., 2019. Permeability enhancement and fracture development of hydraulic in situ experiments in the Äspö Hard Rock Laboratory, Sweden. *Rock Mechanics and Rock Engineering*, *52*(2), pp.495-515.